Dynamic Behavior of Liquids in Elastic Tanks

GHASSAN R. KHABBAZ*
Lockheed Palo Alto Research Laboratory, Palo Alto, Calif.

The finite element procedure is used in conjunction with a simple source distribution on all surfaces of a liquid, which is contained in a tank of virtually arbitrary geometry, to obtain expressions for the mass and stiffness (because of the gravity) matrices of the liquid. The accuracy of the formulation is evaluated by the numerical solution of eigenvalue problems appropriate to simple rigid tanks for which exact analytical solutions are available. Good agreement is obtained. Once the mass and stiffness matrices of the liquid are obtained, they can be combined with those of an elastic tank in order to study the dynamic behavior of liquids in elastic tanks. The matrices for the elastic tank can be generated by any of a variety of currently available finite element or finite difference programs. The dynamic behavior of a liquid in an elastic circular cylindrical tank is treated by making use of a standard finite element program. Very good agreement with the known exact analytical results is obtained. In addition, a tank geometry which cannot be readily analyzed by any of the previously available methods is considered.

Nomenclature

d_n = displacement normal to the surface
g = gravitational acceleration
g_0 = constant in Newton's first law
n = unit vector in the outward normal direction to the surface; also circumferential wave number for shells of revolution
n_z = the z component of n
q_i = + 1 or − 1 relate mirror image in each quadrant
r_{pq} = distance between points p and q
ΔS_i = area associated with node i
T = kinetic energy
U = potential energy
u_i = $\Delta Si/\Delta S_m$ (see Eq. (11))
v_n = velocity normal to the surface
α = $\rho g/2g_0$
θ_{pq} = angle between vector connecting p to q and n at p
ρ = density of liquid
$\sigma(q)$ = source density at point q
$\varphi(p)$ = velocity potential at point p
φ_n = $\partial\varphi/\partial n$
λ = ω^2/g^2

Introduction

PROPELLANT tanks with complex geometries are being considered for next generation space vehicles. Since the fluid has a major impact on the dynamic behavior of the vehicle, it is essential that a method be developed which is practical and useful from an engineering viewpoint for analyzing the dynamic behavior of complex, elastic, liquid-filled tanks.

Previous investigators who used analytical functions to express the dynamic response of liquid-filled tanks were limited in the type of tank geometries they could treat. A few years ago, a finite element formulation for the axisymmetric modes of a hemispherical tank was presented.[1] The approach uses the simple source distribution representation on the surface of the liquid. Nevertheless, the method is restricted to the treatment of one class of problems, namely, axisymmetric modes of shells of revolution. Recently, a nonaxisymmetric finite element method for treating shells of revolution was presented.[2] This approach divides the liquid into triangular annular elements and, therefore, subdivides the entire volume of liquid. Again there is the geometric restriction that only shells of revolution can be analyzed.

At present a number of computer programs are available throughout the country to analyze dry elastic structures. These programs are based on either the finite element or finite difference techniques. The purpose of this work is to extend the capabilities of these programs to enable them to treat liquid-filled tanks with complex geometries. With such capability, the dynamic behavior of elastic, liquid-filled tanks of complex geometry becomes amenable to analysis. In the next section, a brief description of the method is presented.

Technical Approach

At least three different methods can be used to extend the capabilities of finite element and finite difference programs to handle wet structures: 1) Use of a surface source distribution as a basis for the solution (thus, only the surface of the liquid need be considered and a two-dimensional grid results). 2) Subdivision of the total liquid into smaller volumes, which produces a three-dimensional mesh. 3) Representation of liquid behavior by a series of generalized functions weighted by unspecified coefficients.

Method 1 is used since it results in fewer node points than 2, can handle general tank geometries and can be easily incorporated in the existing finite element structural programs.

Derivation of Energy Relations in Terms of Velocity Potential

A simple source distribution on the surface of the liquid is chosen to express the behavior of the liquid. Hence, the velocity potential is expressed as

$$\varphi(p) = \iint \sigma(q) dS/r_{pq} \tag{1}$$

Now one can formulate the equations of motion of the tank-liquid system by writing expressions for the kinetic and potential energies of the system and using Lagrange's principle. Let us restrict our attention to the liquid component since the energy derivation for the elastic component is available in many articles in the open literature.

Received November 19, 1970; revision received May 10, 1971. The work was sponsored by Lockheed's Independent Research fund for 1970. The author is grateful to both C. Coale and T. Geers for their valuable discussions, and to C. Coale and W. Loden for generating the stiffness matrix of the elastic tank. Also thanks are due to J. Vosti for the preparation of the figures.

Index categories: Wave Motion and Sloshing; Structural Dynamics Analysis.

* Research Scientist, Structural Mechanics Laboratory; presently, Vice-President, Karkar Electronics, San Francisco, Calif.

The kinetic energy of the liquid can be expressed as

$$T = (\rho/2g_0)\iint \varphi\varphi_n dS \tag{2}$$

A number of forces such as gravity, surface tension, etc. contribute to the potential energy of the liquid. For the present analysis, we shall restrict our attention to the gravitational effect only. Thus, the change in U is only because of that part of the liquid that leaves the original space. Assume a sinusoidal motion, then the change in volume ΔV through a surface dS is

$$\Delta V = -\varphi_n dS/j\omega \tag{3}$$

One can show[3] that the pertinent term in the potential energy is

$$U = -(\rho g/2g_0\omega^2)\iint \varphi_n{}^2 n_z dS \tag{4}$$

Moreover, for a Lyapunov surface,[4]

$$(\varphi_n)_p = 2\pi\sigma(p) + \iint_{q\neq p}\sigma(q)\cos\theta_{pq}dS/r_{pq}{}^2 \tag{5}$$

Boundary Condition

There are two boundary conditions which must be imposed on the surface of the liquid. 1) Wherever the liquid is in contact with the tank, $(-\varphi_n)$ should be equal to the velocity of the tank in the n direction. 2) The velocity of the liquid normal to its surface cannot be arbitrarily specified. It has to satisfy the incompressibility condition

$$\iint \varphi_n dS = 0 \tag{6}$$

Finite Element Formulation

The energy Eqs. (2) and (4), and the necessary boundary conditions (6), are formulated in terms of φ_n and φ. A finite element approach is used to derive the mass and stiffness matrices in accordance with the following steps: 1) A finite element grid is imposed on all surfaces of the liquid. A node point is associated with each grid element and is located at its center of gravity. The source density distribution is considered constant over each grid element. 2) Equation (5) is reduced to a matrix equation. Then the matrix is inverted in order to express the source density distribution in terms of φ_n. The matrix inversion is expensive for large matrices and a factorization procedure can be used. 3) Equation (1) is reduced to a matrix equation relating the vectors φ to σ. The derivation of the diagonal terms in the above matrix posed an analytical difficulty which had restricted the earlier use of this method. In this paper, an analytical derivation for the diagonal elements appropriate to a general trapezoidal grid is obtained in the Appendix. 4) The energy expressions (2) and (4) are reduced to matrix equations with $(-\varphi_n/j\omega)$ as the variable vector. 5) The kinetic and potential energies are then used to obtain the mass and stiffness matrices. 6) In the case of an elastic shell, the mass and stiffness matrices of the shell are combined with those of the liquid. The eigenvector is expanded to incorporate the additional degrees of freedom of the shell. 7) Finally, the incompressibility condition (6) is imposed.

After the mass and stiffness matrices are obtained, an eigenvalue problem is solved. The over-all solution of the eigenvalue problem consits of finding the eigenvalues, eigenvectors (normal displacement of the liquid surface plus additional shell degrees of freedom), the source density at the node points, and finally the velocity potential. It is known that, at the liquid free surface, the following relation holds: $\varphi_n = \omega^2\varphi/g$. A comparison between the numerical values of φ_n and $\omega^2\varphi/g$ for the various examples showed differences smaller than 2%.

In the remaining part of this section, the details of the finite element formulation are presented. The normal velocity of the liquid surface at the node points is represented by the vector $\mathbf{v_n}$

$$\mathbf{v_n} = -\dot{\boldsymbol{\phi}}_\mathbf{n} = -[C]\dot{\boldsymbol{\sigma}} \tag{7}$$

$$C_{ii} = 2\pi \text{ and } C_{ij} = \cos\theta_{ij}\Delta S_j/r_{ij}{}^2 \tag{8}$$

Then the incompressibility relation Eq. (6) reduces to

$$\mathbf{v_n}{}^T\boldsymbol{\Delta S} = 0 \tag{9}$$

where $\boldsymbol{\Delta S}$ is the vector whose elements are the areas associated with the node points.

This allows the velocity at one node point to be expressed in terms of all the remaining ones; essentially reducing the unknown terms of the problem by one

$$v_{nm} = \mathbf{u}^T\mathbf{v_{n_R}} \tag{10}$$

The original $\mathbf{v_n}$ has m elements. The reduced $\mathbf{v_{n_R}}$ vector has $m - 1$ elements

$$u_i = -\Delta Si/\Delta S_m \tag{11}$$

The velocity potential of Eq. (1) can be written as

$$\dot{\boldsymbol{\phi}} = [\beta]\dot{\boldsymbol{\sigma}} \tag{12}$$

where

$$\beta_{ij} = \Delta S_j/r_{ij} \quad \text{for} \quad i \neq j \tag{13}$$

The expression for β_{ii} is more complicated. It is true that in the limit as ΔS_i becomes small $\beta_{ii} \to 0$, but for the finite mesh areas, β_{ii} is of the same order of magnitude as β_{ij} and cannot be arbitrarily set equal to zero. The derivation for β_{ii} is given in the Appendix.

Substituting Eq. (7) into Eq. (12) gives

$$\dot{\boldsymbol{\phi}} = -[\beta][C]^{-1}\mathbf{v_n} = -[B]\mathbf{v_n} \tag{14}$$

Next the energy expressions will be formulated.

The expression for the potential energy, Eq. (4) can be written as

$$U = -(\rho/2g_0\lambda)\mathbf{v_n}{}^T[A]\mathbf{v_n} \tag{15}$$

where $[A]$ is a diagonal matrix whose elements are

$$A_{ii} = \Delta S_i(n_{iz}) \tag{16}$$

and n_{iz} is n_z at node i.

By making use of Eqs. (14) and (2), the expression for the kinetic energy can be expressed as

$$T = (\rho/2g_0)\mathbf{v_n}{}^T[B]\mathbf{v_n} \tag{17}$$

Since harmonic motions are being considered, one can easily express the kinetic and potential energies in terms of displacements instead of velocities. Then substituting Eqs. (15) and (17) in Lagrange's equation yields

$$\alpha\{[A]^T + [A] - \lambda([B]^T + [B])\}\mathbf{d_n} = 0 \tag{18}$$

From Eq. (18) it can be seen that the stiffness matrix is $\alpha([A]^T + [A])$ and the mass matrix is $\alpha([B]^T + [B])$. To incorporate the incompressibility, Eq. (6) can be introduced into Eq. (18) through the matrix $[D]$.

$$\alpha[D]^T\{[A]^T + [A] - \lambda([B]^T + [B])\}[D]d_n = 0 \tag{19}$$

where D is a $(m - 1) \times m$ matrix whose diagonal elements are unity. The off-diagonal elements are zero except for D_{im} when i is not in contact with a rigid tank. Then

$$D_{im} = -\Delta S_i/\Delta S_m = u_i \tag{20}$$

Let

$$V = [D]^T[A][D] \tag{21}$$

and

$$W = [D]^T[B][D] \tag{22}$$

Then Eqs. (21) and (22) reduce to

$$\alpha\{[V]^T + [V] - \lambda([W]^T + [W])\}\mathbf{d_n} \qquad (23)$$

Equation (23) is the eigenvalue formulation for the slosh in a rigid container. To include the stiffness and mass matrices of the elastic tank, one has to return to Eq. (18). Overlay the mass and stiffness matrices of the elastic tank over those of the liquid while expanding the eigenvector to include all the degrees of freedom of the shell. Note that where the liquid is in contact with the tank the normal deflection of the tank is the same as d_n. This is the general formulation of the problem.

Note that if k refers to an in-plane degree of freedom of the shell, then

$$D_{ki} = D_{ik} = 0 \qquad \text{if } k \neq i \qquad (24)$$

For special types of tanks advantages can be made of planes of symmetry or the fact that the tank is a shell of revolution.

Two Planes of Symmetry

If the tank has two planes of symmetry, then only one-fourth of the tank needs to be analyzed. Terms such as source density distribution, normal velocity and velocity potential in the second, third, and fourth quadrants will be expressed in terms of those in the first quadrant.

Let the four quantities q_i, $i = 1, 4$ relate the mirror image of what happens in the first quadrant to the remaining three. If $q_1 = +1$, then by specifying q_i (for $i = 2,3,4$) either $+1$ or -1, we can obtain all possible modes.

Denote with $*$ expressions when one analyzes a quarter tank

$$C_{ii}^* = C_{ii} + \Delta S_i \sum_{k=2}^{4} q_k \cos\theta_{ik}/r_{ik}^2 \qquad (25a)$$

$$\beta_{ii}^* = \beta_{ii} + \Delta S_i \sum_{k=2}^{4} q_k/r_{ik} \qquad (25b)$$

where point k is the mirror image of point i in the kth quadrant.

$$C_{ij}^* = \Delta S_j \sum_{k=1}^{4} q_k \cos\theta_{ik}/r_{ik}^2 \qquad (26a)$$

$$\beta_{ij}^* = \Delta S_j \sum_{k=1}^{4} q_k/r_{ik} \qquad (26b)$$

where point k is the mirror image of point j in the kth quadrant. Finally

$$A_{ij}^* = A_{ij} \qquad (27)$$

The eigenvalue problem reduces to

$$\alpha\{[A^*]^T + [A^*] - \lambda([B^*]^T + [B^*])\}\mathbf{d_n}^* = 0 \qquad (28)$$

The incompressibility condition needs to be forced through the use of matrix D only when all the q_i's are positive. When two of the q_i's are positive and the remaining two are negative, incompressibility is automatically enforced.

Shells of Revolution

For tanks having the geometry of shells of revolution, advantage can be taken of the fact that the mode shapes in the circumferential direction are expressed in terms of an orthogonal series $\cos n\theta$ or $\sin n\theta$. This reduces the finite element from a 2-D problem to 1-D allowing a finer mesh for the same number of node points and a more accurate determination of the eigenvalues and mode shapes. Let us choose a grid system where the node points lie on the $\theta = 0$ axis. Denote with superscript-expressions for shells of revolution, then

$$\bar{C}_{ii} = C_{ii} + \Delta S_i \sum_{k=2}^{K} \cos\theta_{ik} \frac{F_{nk}}{r_{ik}^2} \qquad (29a)$$

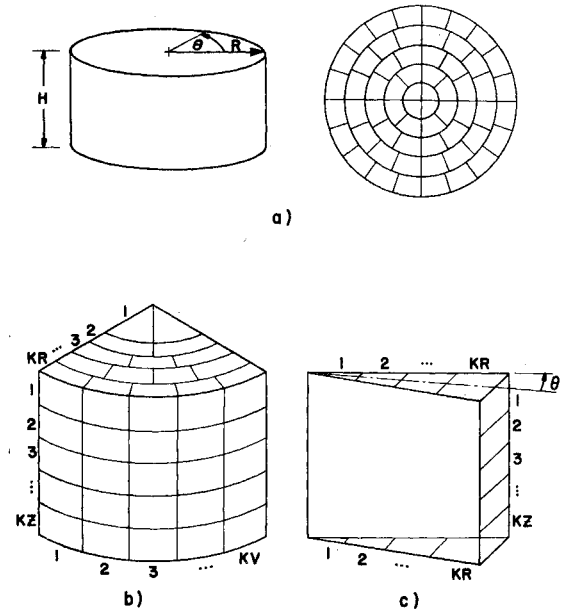

Fig. 1 Circular cylindrical tank: a) complete cylinder; b) quarter model grid system; c) grid system for shell of revolution model.

$$\bar{\beta}_{ii} = \beta_{ii} + \Delta S_i \sum_{k=2}^{K} \frac{F_{nk}}{r_{ik}} \qquad (29b)$$

where

$$F_{nk} = \cos 2\pi n(k-1)/K \qquad (30)$$

K is the number of partitions in the θ (circumferential direction). Points k are in the same θ plane as node i, i.e., where the other two coordinates are constant equal to those of i. Also

$$\bar{C}_{ij} = \Delta S_j \sum_{k=1}^{K} \cos\theta_{ik} \frac{F_{nk}}{r_{ik}^2} \qquad (31a)$$

$$\bar{\beta}_{ij} = \Delta S_j \sum_{k=1}^{K} \frac{F_{nk}}{r_{ik}} \qquad (31b)$$

where F_{nk} is the same as in Eq. (30), but now the points k are in the same θ plane as node j. Note that for $k = 1$ we get node j. Finally

$$\bar{A}_{ij} = A_{ij} \qquad (32)$$

The eigenvalue problem reduces

$$\alpha\{[\bar{A}]^T + [\bar{A}] - \lambda([\bar{B}]^T + [\bar{B}])\}\bar{\mathbf{d}}_n = 0 \qquad (33)$$

The incompressibility condition needs to be forced through the use of matrix $[D]$ only for $n = 0$, i.e., for the axisymmetric node.

Numerical Results

First, a simple example that has been solved analytically is used to demonstrate the accuracy and evaluate the convergence of the present method. Then a rigid tank with complex geometry, which cannot be readily treated by any of the previously available methods, is analyzed. Finally, an elastic tank with simple geometry is analyzed. This is done in order to illustrate that dynamic behavior of liquids in elastic tanks can be studied by combining the mass and stiffness matrices of the liquid as derived here with those obtained for an elastic shell from the available finite element or finite difference programs.

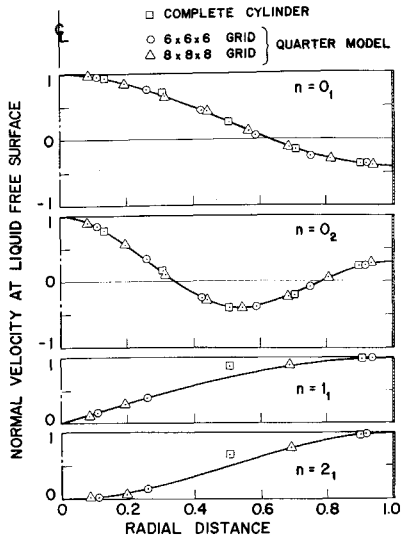

Fig. 2 Rigid circular cylindrical tank $H/R = 1$; variation of liquid normal velocity at free surface with radial distance.

Rigid Circular Cylindrical Tank

First, the simple example of the rigid circular cylindrical tank with a flat bottom is treated. Three different models are used for the analysis. The purpose of choosing the three models is to show that although the program can treat tanks of general geometry, it can easily be specialized to take advantage of planes of symmetry or of the known circumferential variation for modes of shells of revolution. Figures 1 illustrate the grid associated with the three aforementioned models.

1) *Complete tank model* Identical grids are chosen for the top and bottom liquid surfaces as shown in Fig. 1a. Each grid possesses sixty node points. The cylindrical surface is divided into ten identical circumferential divisions and five identical axial subdivisions. This produces 50 node points.

2) *Quarter model* The grid for the quarter model is shown in Figure 1b. It is described by the dimension $KR \times KZ \times KV$ as indicated in Fig. 1b.

3) *Shell of revolution model* For the shell of revolution model, the node points are chosen to fall on $\theta = 0$ lines. The grid is designated by $KR \times KZ \times K$ as indicated in Fig. 1c. The parameter K is the circumferential number of partitions, see Eq. (30).

One grid size is used for each of the complete cylinder and shell of revolution models, while a number of different grid sizes are evaluated for the quarter model. The purpose of this is to illustrate the validity of the program for the complete cylinder and shell of revolution models while studying

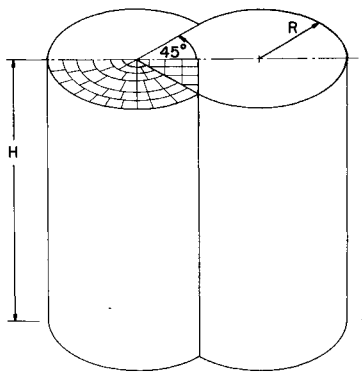

Fig. 3 Double lobed cylindrical tank; shown is the grid mesh on upper flat surface for quarter model.

Table 1 Slosh eigenvalues ($\omega^2 R/g$) in a rigid circular cylindrical tank $H/R = 1.0$

		Finite element 2-D					3-D Finite element Ref. 2
		Complete cylinder	Quarter Model			Shell of rev	
n[a]	Exact		6×6×6	7×7×7	8×8×8	10×10×40	
1_1	1.750	2.0730	1.7448	1.7385	1.7344	1.7602	
2_1	3.0542	3.5787	3.0649	3.0494	3.0385	3.0784	
0_1	3.8317	4.2004	4.0844	4.0230	3.9886	3.8714	3.83
3_1	4.2012	4.9548	4.2785	4.2565	4.2385	4.2795	
4_1	5.3176	6.2343	5.4386	5.4187	5.3989	5.4495	
1_2	5.3314	5.9341	5.5947	5.5556	5.5241	5.4180	
5_1	6.4156	7.1066	6.5476	6.5488	6.5364	...	
2_2	6.7061	7.4380	7.0806	7.0379	6.9983	6.9021	
0_2	7.0156	7.8349	7.6498	7.5687	7.5038	7.0879	7.30
6_1	7.5013		...	7.639	7.6462	...	
3_2	8.0152		8.4422[b]	8.4577	8.4308	8.3323	
1_3	8.5363		9.1422	9.1042	9.070	8.6794	

[a] n = circumferential wave number; subscript on n is the radial mode index.
[b] Eigenvalue not definitely identified with the mode shape.

the convergence vs grid size on the quarter model. A more detailed study of the quarter model is undertaken because only a quarter model of the double-lobed tank is studied later on. Table 1 shows a comparison of the eigenvalues as obtained by the previous models with those obtained from the exact analysis and the finite element method of Ref. 2.

For the complete cylindrical model, there are two identical eigenvalues for each $n \neq 0$; where n is the circumferential wave number. One of these corresponds to the $\cos n\theta$ and the other to the $\sin n\theta$ variation. The numerical difference between the calculated eigenvalues is less than 0.3% for the same n. The average of these two values is presented in the third column of Table 1. The radial variation of the liquid normal velocity at the free surface is shown in Fig. 2. The points are the numerical results and the solid line is from the analytical closed form solution using Bessel functions. The comparison between the numerical results and $\cos n\theta$ for the circumferential variation compared even better than the points and solid line of Fig. 2.

From studying the results, it can be seen that the eigenvalues for the complete cylindrical model are off by as much as 18%, i.e., the frequency is off by 9%. Moreover, although the mode shapes from this model have the same patterns as the exact ones, they are not identical. This leads to the conclusion that the grid is too coarse. The variation of the first two eigenvalues with grid size for the quarter model indicates that once a grid size is obtained for which the eigenvalue converges to the exact one, a further refinement in the grid causes a slight decrease in the eigenvalues of the order of half a %. This can be attributed to numerical errors. By looking at modes higher than the second, one can observe the convergence of the eigenvalues to the exact solution for a finer grid size. In this work, a simple finite element formulation of Eq. (1) is used as expressed by Eq. (12). This makes it necessary to use grid elements of nearly unit aspect ratio. Errors will be introduced if the mesh element is very thin and no convergence will result. Actually an interesting problem for future investigation is to use a more developed finite element formulation of Eq. (1) and avoid the nearly unit aspect ratio restriction.

Figure 2 shows a comparison of the mode shapes for the various models and grids with those of the exact solution. Actually, even for the $6 \times 6 \times 6$ grid, results for the first few modes are very good. Finally, the eigenvalues for the shell of revolution model are also presented in Table 1. Although for this latter model, separate computer runs had to be made for each circumferential wave number, the time for each run is nearly an order of magnitude less than that for the quarter model having the same distance between the node points. For the grid in Table 1 of the shell of revolution model, it takes nearly 10 sec on the UNIVAC 1108 to obtain the first three eigenvalues, eigenvectors, and velocity potential for each circumferential wave number.

Table 2 Slosh eigenvalues (ω^2R/g) in a rigid double lobed cylindrical tank $H/R = 1.0$

Mode number	ω^2R/g	Remarks	q_1	q_2	q_3	q_4
1	0.8167	Rocking around x-x axis	+1	−1	−1	+1
2	1.8079	Rocking around y-y axis	+1	+1	−1	−1
3	2.0494	Fig. 4	+1	+1	+1	+1
4	2.8656	"	+1	−1	−1	+1
5	3.2893	"	+1	+1	−1	−1
6	3.5008	"	+1	+1	+1	+1
7	4.0350	"	+1	−1	−1	+1
8	4.1217	"	+1	+1	+1	+1

Double-Lobed Cylindrical Tank

Then a tank which cannot easily be analyzed by any of the previously available methods is treated. A quarter model is chosen as shown in Fig. 3. The mesh shown in Fig. 3 is that taken for the top and bottom flat surfaces. The cylindrical curved sides are divided into ten equal circumferential parts and six equal axial divisions. The total number of node points on all the surfaces was 150, of which 45 were on the liquid free surface. The mesh size is comparable to that of a circular cylindrical tank with a grid $6 \times 6 \times 6$. Again frequencies, mode shapes, and comparison of φ_n and $\omega^2\varphi/g$ at the free surface of the liquid were calculated. Table 2 gives the eigenvalues for the first eight mode shapes. In Fig. 4 the modes are shown schematically. The shaded and clear areas represent motion of the free surface upward and down, respectively.

Elastic Circular Cylindrical Tank with a Flat-Rigid- Fixed Bottom

This particular example was chosen to illustrate that the mass and stiffness matrices of the liquid can be combined with those for the elastic shell as obtained by any finite element or finite difference program in order to study the dynamic behavior of liquids in elastic tanks. A flexible circular cylindrical tank with a rigid bottom is chosen for the example. The boundary conditions used are axial and tangential motions are zero at the bottom and all the degrees of freedom are unrestricted at the upper end of the shell. The mass of the shell was neglected for no reason other than to compare with the results of Ref. 5. A quarter model was chosen and the finite element grid similar to that in Fig. 1 was chosen. For the particular parameters which are chosen for the tank, the modes can be divided into two types: 1) *Slosh modes*—where the surface of the liquid sloshes around while the sides of the tank hardly move. Actually, the computer program gives radial tank deflections a couple of orders of magnitude smaller than the normal motion of the liquid at the free surface. For these modes, the eigenvalues and vectors are very close to those in which the tank is considered rigid. 2) *Elastic modes*—where both the liquid free surface motion and the radial deflection of the tank walls are of the same order of magnitude.

Table 3 Eigenvalues ($R\omega^2/g$) for the elastic cylindrical tank $H/R = 3$

Mode	Exact	Ref. 6	Present Analysis
n			
2_S[a]	3.0542		3.232
0_S	3.8317		4.079
4_S	5.3176		5.3515
0_S	7.0156		6.824
2_E			23.03
0_E		143	146.9
2_E			335.0
0_E		1020	1053
2_E			1252
0_E		2220	2145

[a] Subscript S for slosh modes.
[b] Subscript E for elastic modes.

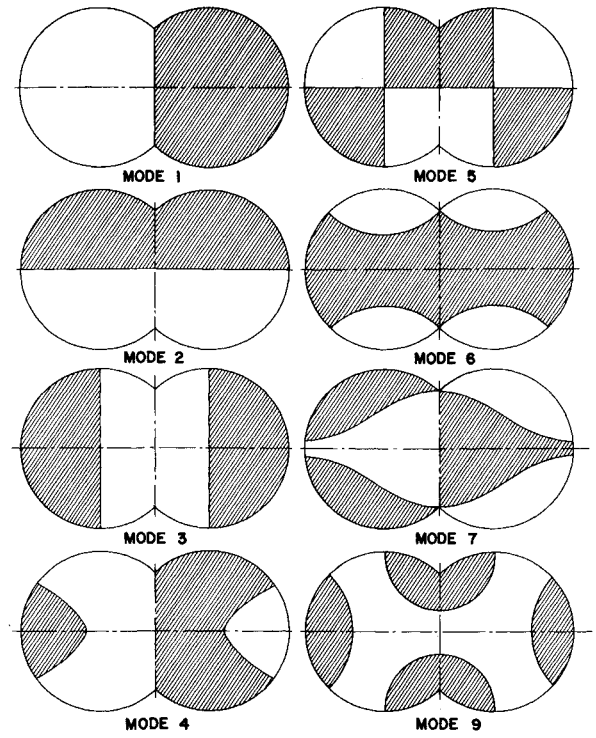

Fig. 4 Double lobed cylindrical rigid tank modes $H/R = 1$; normal motion at liquid free surface; shaded motion up, clear motion down.

The eigenvalues for $n = 0$ and $n = 2$ and comparison with available exact analytical solutions are given in Table 3. The radial deflection for the first two axisymmetric elastic modes are shown in Fig. 5. Excellent agreement is obtained for the first three axisymmetric elastic eigenvalues. The slosh eigenvalues as obtained from this model are not as good as those obtained from the previous model for the rigid tank. This is due to the fact that only few node points are taken on the free surface of the liquid in the present model.

Finally, it should be noted that the finite element and finite difference programs have node points at the edges of the structure in addition to the interior domain. On the other hand, the node points of the fluid element are at the center of gravity of the grid element, thus never on the edges. A transformation is needed to change the mass and stiffness matrices of the structure so that the node points of the structure correspond to those of the fluid. A transformation is used which makes the energy invariant[3] for the two different node systems.

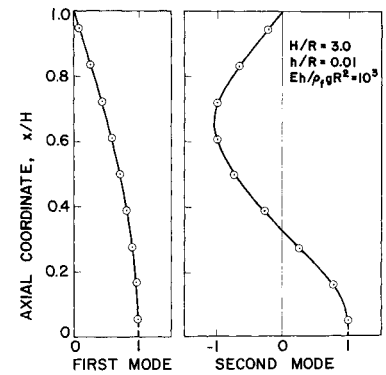

Fig. 5 Radial displacement for the massless cylindrical tank for $n = 0$.

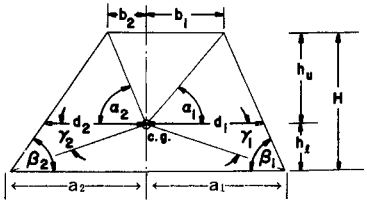

Fig. 6 Trapezoidal element.

Conclusion

The problem of the dynamic behavior of liquids in elastic tanks of general geometry has been formulated and a computer program developed. The main analytical difficulty is in calculating the diagonal terms of the matrix that relates the velocity potential to the source distribution. A closed-form expression for this term in the case of trapezoidal grid elements is derived.

The contribution of this paper is that it derives the mass and stiffness matrices for the liquid in a tank of practically any geometry. The accuracy of the mass and stiffness matrices is evaluated through the solution of eigenvalue problems for rigid tanks and comparing the results with known exact analytical results which are available. It is demonstrated that these matrices are accurately calculated. Finally, the mass and stiffness matrices of the liquid can be combined with those obtained for the elastic tank by any of the available finite element or finite difference programs to study the dynamic behavior of liquids in elastic tanks. To illustrate this last point, the dynamic behavior of an elastic tank containing liquid is investigated, by combining the liquid element analysis of this paper and a standard finite element program for the elastic tank. Excellent agreement with the known exact analytical results[5] are obtained.

Appendix: Contribution to the Velocity Potential at a Node from the Mesh Area Associated with that Node

The velocity potential is expressed in terms of the source distribution in Eq. (1). The finite element formulation is given in Eq. (12). In this appendix, we are calculating β_{ii}, i.e., β_{ij} when $i \to j$. One can think of β_{ii} as the velocity potential at the center of the mesh area ΔS_i because of a constant uniform source density of unit value. Hence

$$\beta_{ii} = \int dS/r = \iint r dr d\theta/r = \iint dr d\theta = \int r d\theta \qquad \text{(A1)}$$

As a general case, consider a trapezoid to represent a mesh area, Fig. 6. Such a trapezoid can be reduced to a number of special areas by the proper choice of the parameters a_i, b_i, and H. For example, for $a_1 = a_2 = b_1 = b_2$, one has a rectangular mesh, and for $b_1 = b_2 = 0$, one has a triangular grid. To perform the integration $\int r d\theta$, we break the trapezoid into two parts; those designated by subscript 1 and those by subscript 2. Each part is then divided into two elements, I above the c.g. and II below the c.g. The contribution to the integration from element I is $(b_i \sin\beta_i + h_u \cos\beta_i) \ln(\tan\alpha_i/2 + \tan\beta_i/2)/[(\tan\beta_i/2)(1 - \tan\beta_i/2 \tan\alpha_i/2)] - h_u \ln(\tan \alpha_i/2)$ and from element II is $d_i \sin\beta_i \ln[(\tan\beta_i/2)(1 + \tan\beta_i/2 \tan\gamma_i/2)/(\tan\beta_i/2 - \tan\gamma_i/2) - h_l \ln(\tan \gamma_i/2)$. Then the integration for the whole trapezoid will be the contribution from element I plus that from element II for both $i = 1,2$.

References

[1] Guyan, R. J., Ujihara, B. H., and Welch, P. W., "Hydroelastic Analysis of Axisymmetric Systems by a Finite Element Method," 2nd Conference on Matrix Methods in Structural Mechanics, Oct. 1968, Wright-Patterson Air Force Base, Ohio.

[2] Luk, C.-H., "Finite Element Analysis for Liquid Sloshing Problems," AFOSR 69-1504TR, ASRL TR-144-3, May 1969, Aeroelastic and Structures Research Lab., MIT, Cambridge, Mass.

[3] Khabbaz, G. R., "Dynamic Behavior of Liquids in Elastic Tanks," LMSC 60-80-70-23, Aug. 1970, Lockheed Missiles & Space Co.

[4] Sobolev, S. L., *Partial Differential Equations of Mathematical Physics*, Pergamon Press, New York, p. 212.

[5] Beal, T. R., Coale, C. W., and Nagano, M., "Influence of Shell Inertia and Bending Stiffness on the Axisymmetric Modes of a Partially-Filled Cylindrical Tank," LMSC 6-75-65-33, Lockheed Missiles & Space Co.